

## What can we learn from the irregularity of $\text{Ca}^{2+}$ oscillations?

Geneviève Dupont<sup>1</sup> and Laurent Combettes<sup>2</sup>

<sup>1</sup>Unité de Chronobiologie Théorique, Faculté des Sciences, Université Libre de Bruxelles, Campus Plaine CP231, Boulevard du Triomphe, B-1050 Brussels, Belgium

<sup>2</sup>Unité UMR-S757, Institut National de la Santé et de la Recherche Médicale,

<sup>3</sup> Université Paris-Sud, F-91405 Orsay, France

(Received 20 February 2009; accepted 7 June 2009; published online 18 September 2009)

In most cells,  $\text{Ca}^{2+}$  increases in response to external stimulation are organized in the form of oscillations and waves that sometimes propagate from one cell to another. Numerous experimental and theoretical studies reveal that this spatiotemporal organization contains a non-negligible level of stochasticity. In this study, we extend the previous work based on a statistical analysis of experimental  $\text{Ca}^{2+}$  traces in isolated, hormone-stimulated hepatocytes and on stochastic simulations of  $\text{Ca}^{2+}$  oscillations based on the Gillespie's algorithm. Comparison of the coefficients of variation in the periods of experimental and simulated  $\text{Ca}^{2+}$  spikes provides information about the clustering and the specific subtypes of the  $\text{Ca}^{2+}$  channels. In hepatocytes coupled by gap junctions, the global perfusion with a hormone leads to successive  $\text{Ca}^{2+}$  responses, giving the appearance of an intercellular wave. Statistical analysis of experimental  $\text{Ca}^{2+}$  oscillations in coupled hepatocytes confirms that this coordinated  $\text{Ca}^{2+}$  spiking corresponds to a phase wave but suggests the existence of an additional coupling mechanism. © 2009 American Institute of Physics. [DOI: 10.1063/1.3160569]

**Changes in  $\text{Ca}^{2+}$  concentration represent one of the most widespread and versatile signaling pathways. These elevations of  $\text{Ca}^{2+}$  are observed at very different time and length scales, depending on the nature and the intensity of the stimulus, giving rise to very specific physiological responses.<sup>1</sup> Much of this specificity can be ascribed to the spatiotemporal organization of  $\text{Ca}^{2+}$  dynamics as the signaling versatility of this messenger can be exploited to regulate diverse cellular responses. For example, the extent of the physiological response of the cell is in many cases encoded in the frequency of  $\text{Ca}^{2+}$  oscillations. Increasing the extent of stimulation indeed induces a rise in the frequency of oscillations, as well as a higher level of the  $\text{Ca}^{2+}$ -mediated physiological response. It is thus vital for the cell that  $\text{Ca}^{2+}$  dynamics is robust and reproducible. In the present study, we investigate this regularity on the basis of experimental time series of noradrenaline-induced  $\text{Ca}^{2+}$  oscillations in isolated hepatocytes. These results are related to stochastic simulations to gain insight into the molecular mechanisms underlying this repetitive spiking. Extension of the statistical analysis to cells coupled by gap junctions sheds light on the phase wave mechanism responsible for the observed coordination of  $\text{Ca}^{2+}$  spiking.**

### I. INTRODUCTION

$\text{Ca}^{2+}$  oscillations mainly occur through periodic exchanges of  $\text{Ca}^{2+}$  between the endoplasmic reticulum (ER) and the cytoplasm.<sup>1</sup> This release is initiated by inositol 1,4,5-trisphosphate ( $\text{InsP}_3$ ) synthesized by phospholipase C (PLC) in response to external stimulation. The  $\text{InsP}_3$  receptor ( $\text{InsP}_3\text{R}$ ) located in ER membrane is a channel allowing the flux of  $\text{Ca}^{2+}$  down to its electrochemical gradient.  $\text{Ca}^{2+}$  concentrations in the ER and in the cytosol are indeed strikingly

different: 500  $\mu\text{M}$  in the ER versus 0.1  $\mu\text{M}$  in the cytoplasm. Because the  $\text{InsP}_3\text{R}$  is highly regulated and because there are also active  $\text{Ca}^{2+}$  pumps in the ER membrane, quite regular  $\text{Ca}^{2+}$  oscillations arise in many cell types for a finite range of stimulation levels.

In cells exhibiting  $\text{Ca}^{2+}$  oscillations, subthreshold stimulations in contrast induce localized and short-lived  $\text{Ca}^{2+}$  increases that are stochastic by nature as they involve a low number of  $\text{Ca}^{2+}$  channels.<sup>2,3</sup> In this case, the description of  $\text{Ca}^{2+}$  dynamics must be both stochastic and microscopic as theoretical studies suggest that cytosolic and luminal depletion domains alter the gating of  $\text{Ca}^{2+}$ -regulated  $\text{Ca}^{2+}$  channels.<sup>4-6</sup> For the passage to whole cell  $\text{Ca}^{2+}$  oscillations, two different scenarios can thus be envisaged. First, the increase in the level of stimulation could allow the passage from a stochastic to a deterministic regime due to the increasing number of channels participating in the dynamics of  $\text{Ca}^{2+}$  responses. Second, it is possible that the cytoplasm always behaves as a stochastic medium with more or less regular spikes corresponding to the regime of array enhanced coherence resonance.<sup>7</sup> This last hypothesis is corroborated by the observation that in some cell types, the standard deviation of the interspike interval is of the order of the mean interspike interval.<sup>8</sup> However, this is not the case in all cell types. In hepatocytes, for example, the coefficient of variation (CV) in the period lies in the 10%–15% range.<sup>9</sup> This level of regularity can be accounted for by a deterministic oscillatory regime perturbed by internal noise.

In such a regime, some information can be gained from the irregularity of the spikes. For example, fluctuations on the period provide information about the extent of channel clustering. In a hepatocyte stimulated by noradrenaline, the CV of the period lies in the 10%–15% range and is due to the molecular fluctuations. During hormone-induced  $\text{Ca}^{2+}$  oscil-

lations,  $\text{Ca}^{2+}$  is released from the ER through  $\text{InsP}_3$  receptors/ $\text{Ca}^{2+}$  channels ( $\text{InsP}_3\text{Rs}$ ). On the basis of the known density of  $\text{InsP}_3$  binding sites,<sup>10</sup> the number of these receptors present in one hepatocyte is estimated to about 6000. To account for the 10%–15% CV, simulations based on the Gillespie's algorithm predict that channels must be clustered in groups of  $\sim 25$  closely packed entities, in fact behaving as “megachannels.”<sup>9</sup> This notion of clustering of  $\text{Ca}^{2+}$  channels is in agreement with the results from simulations of the smaller-scale  $\text{Ca}^{2+}$  increases at subthreshold stimulation levels known as  $\text{Ca}^{2+}$  puffs.<sup>7,11,12</sup> CVs of the periods are not only governed by the level of channel clustering, they are also related to the receptor subtypes. Three isoforms of the  $\text{InsP}_3\text{R}$  differing among other factors by their regulatory properties by  $\text{Ca}^{2+}$  and  $\text{InsP}_3$  have been identified.<sup>13,14</sup> Because of different kinetics, these subtypes are distinctly affected by the molecular noise, which may explain the various levels of regularity of the oscillatory  $\text{Ca}^{2+}$  dynamics observed in the different cell types.<sup>9,15</sup>

In the present study, we first review and extend the analysis summarized above. We also analyze  $\text{Ca}^{2+}$  oscillations in cells coupled by gap junctions. In such connected cells, the global perfusion with a hormone leads to successive  $\text{Ca}^{2+}$  responses in adjacent cells, giving the appearance of an intercellular wave.<sup>16,17</sup> This coordinated spiking in small groups of hepatocytes (called “doublets” or “triplets”) is reminiscent of the  $\text{Ca}^{2+}$  waves that can invade a whole liver lobule.<sup>18</sup> Coordination of  $\text{Ca}^{2+}$  increases at the organ level may have significant physiological implications in relationship to bile secretion, glucose output, or liver regeneration.<sup>19</sup> Previous modeling studies from our group suggest that experimental observations about  $\text{Ca}^{2+}$  spikes in doublets and triplets are best accounted for when assuming that  $\text{Ca}^{2+}$  oscillations in adjacent cells are not synchronized but rather coordinated by a phase wave propagation mechanism. This phase wave originates from the different sensitivities of the cells to the hormonal stimulus together with the passage of  $\text{InsP}_3$  through gap junctions.<sup>20,21</sup> Here, we perform a statistical analysis of the regularity of the period in connected hepatocytes that confirms this phase wave hypothesis and also suggests the existence of an additional mechanism adjusting the timing of the  $\text{Ca}^{2+}$  peaks in adjacent cells.

## II. MATERIAL AND METHODS

### A. Computation: Simulations based on the Gillespie's algorithm of the intracellular $\text{Ca}^{2+}$ dynamics in hepatocytes

As in most cell types, hormonal stimulation of hepatocytes leads to the activation of PLC, an enzyme that catalyzes the synthesis of inositol 1,4,5-trisphosphate ( $\text{InsP}_3$ ). This messenger binds to receptors located on the surface of the ER, which are at the same time  $\text{Ca}^{2+}$  channels. Thus, an increase in  $\text{InsP}_3$  concentration brings about a release of  $\text{Ca}^{2+}$  from the ER into the cytosol. The oscillatory mechanism relies on the autocatalytic regulation exerted by cytosolic  $\text{Ca}^{2+}$  on the  $\text{InsP}_3\text{R}$ . Release terminates when cytosolic  $\text{Ca}^{2+}$  levels get close to concentrations that could be detrimental to the cell as the  $\text{InsP}_3\text{R}$  becomes inhibited. Experiments show-

ing this bell-shaped dependence of the open probability of this channel as a function of cytosolic  $\text{Ca}^{2+}$  are well known.<sup>22,23</sup> ATPases pump  $\text{Ca}^{2+}$  from the cytosol back in the ER. Various mathematical models based on this core oscillatory mechanism have been proposed (see Ref. 24 for a recent review). While some models use an empirical description of the successive positive and negative feedbacks leading to oscillations,<sup>25–27</sup> mechanistic models describe in a more realistic way the transitions between the states of the receptor channel.<sup>28,29</sup> It should also be mentioned that besides  $\text{InsP}_3\text{R}$  regulation, some models take into account other phenomena related to  $\text{InsP}_3$  and/or  $\text{Ca}^{2+}$  dynamics that markedly influence  $\text{Ca}^{2+}$  oscillations and waves in some cell types. Thus,  $\text{Ca}^{2+}$  feedbacks at the level of  $\text{InsP}_3$  synthesis or metabolism into  $\text{InsP}_2$  or  $\text{InsP}_4$  can markedly influence the time evolution of  $\text{Ca}^{2+}$  and  $\text{InsP}_3$ .<sup>30–33</sup> Because  $\text{Ca}^{2+}$  is electrically charged, ER membrane potential oscillations can also be considered.<sup>34</sup> The fact that  $\text{Ca}^{2+}$  enters the cytosol both from the ER and from the external medium makes the understanding of the observed  $\text{Ca}^{2+}$  dynamics significantly more difficult and has also been considered in some models.<sup>33,35</sup> Finally,  $\text{Ca}^{2+}$ -activated protein kinase C (Refs. 36 and 37) or phosphorylation of the  $\text{InsP}_3\text{R}$  (Ref. 38) has been shown to affect the rate of  $\text{InsP}_3$  synthesis and thus  $\text{Ca}^{2+}$  dynamics after stimulation of some types of PLC-linked external receptors.

Our stochastic numerical procedure used to simulate  $\text{Ca}^{2+}$  oscillations describes the transitions between the various states of the  $\text{InsP}_3\text{R}$ . The receptor/channel has two binding sites, one for activating  $\text{Ca}^{2+}$  and one for inhibiting  $\text{Ca}^{2+}$ . Each binding site can accommodate 2  $\text{Ca}^{2+}$  ions. Thus, nine states represented by the different combinations  $R_{ij}$  ( $i$  and  $j$  varying from 0–2) are considered. The  $\text{InsP}_3\text{R}$  also possesses one binding site for  $\text{InsP}_3$ , but this binding-dissociation process is assumed to be at quasiequilibrium. The model also considers a Hill term for  $\text{Ca}^{2+}$  entry in the ER and a linear leak term. All these processes are simulated on the basis of the Gillespie's algorithm.<sup>39</sup> A list of all possible transitions is given in Table I. A detailed description of the model can be found in Ref. 9. Parameters values are listed in Table II.

## B. Experiments

### 1. Materials

Williams' medium was from Life Technology (Invitrogen, Cergy-pontoise, France), Collagenase A from Boehringer (Roche Diagnostics, Meylan, France). Other chemicals were purchased from Sigma (Sigma-Genosys, Sigma-Aldrich Chimie, St. Quentin Fallavier, France).

### 2. Hepatocyte preparation

Hepatocytes were prepared from fed female Wistar rats by limited collagenase digestion of rat liver, as previously described.<sup>21</sup> Experiments were conducted according to the CEE directives for animal experimentation (decree 2001-131; “J.O.” 06/02/01). After isolation, rat hepatocytes were maintained ( $2.10^6$  cells/mL) at 4 °C in Williams medium E supplemented with 10% fetal calf serum, penicillin (200 000 U/mL), and streptomycin (100 mg/mL). Cell viability, assessed by trypan blue exclusion, remained at >96% for 4 and 5 h.

TABLE I. Stochastic model for Ca<sup>2+</sup> oscillations based on the Gillespie's algorithm. The first column lists the sequence of reactions; the probability of each reaction is given in the second column. The last column indicates the changes in the number of molecules/ions taking part in the different reactions.  $\Omega$  allows modulating the number of molecules present in the cytoplasm and in the ER.

Reaction step	Probability	Changes in particle numbers
$R_{00} + C \rightarrow R_{10}$	$k_{a1+} \times C \times R_{00} / \Omega$	$R_{00} \rightarrow R_{00} - 1; R_{10} \rightarrow R_{10} + 1; C \rightarrow C - 1$
$R_{10} \rightarrow R_{00} + C$	$k_{a1-} \times R_{10}$	$R_{10} \rightarrow R_{10} - 1; R_{00} \rightarrow R_{00} + 1; C \rightarrow C + 1$
$R_{10} + C \rightarrow R_{20}$	$k_{a2+} \times C \times R_{10} / \Omega$	$R_{10} \rightarrow R_{10} - 1; R_{20} \rightarrow R_{20} + 1; C \rightarrow C - 1$
$R_{20} \rightarrow R_{10} + C$	$k_{a2-} \times R_{20}$	$R_{20} \rightarrow R_{20} - 1; R_{10} \rightarrow R_{10} + 1; C \rightarrow C + 1$
$R_{01} + C \rightarrow R_{11}$	$k_{a1+} \times C \times R_{01} / \Omega$	$R_{01} \rightarrow R_{01} - 1; R_{11} \rightarrow R_{11} + 1; C \rightarrow C - 1$
$R_{11} \rightarrow R_{01} + C$	$k_{a1-} \times R_{11}$	$R_{11} \rightarrow R_{11} - 1; R_{01} \rightarrow R_{01} + 1; C \rightarrow C + 1$
$R_{11} + C \rightarrow R_{21}$	$k_{a2+} \times C \times R_{11} / \Omega$	$R_{11} \rightarrow R_{11} - 1; R_{21} \rightarrow R_{21} + 1; C \rightarrow C - 1$
$R_{21} \rightarrow R_{11} + C$	$k_{a2-} \times R_{21}$	$R_{21} \rightarrow R_{21} - 1; R_{11} \rightarrow R_{11} + 1; C \rightarrow C + 1$
$R_{02} + C \rightarrow R_{12}$	$k_{a1+} \times C \times R_{02} / \Omega$	$R_{02} \rightarrow R_{02} - 1; R_{12} \rightarrow R_{12} + 1; C \rightarrow C - 1$
$R_{12} \rightarrow R_{02} + C$	$k_{a1-} \times R_{12}$	$R_{12} \rightarrow R_{12} - 1; R_{02} \rightarrow R_{02} + 1; C \rightarrow C + 1$
$R_{12} + C \rightarrow R_{22}$	$k_{a2+} \times C \times R_{12} / \Omega$	$R_{12} \rightarrow R_{12} - 1; R_{22} \rightarrow R_{22} + 1; C \rightarrow C - 1$
$R_{22} \rightarrow R_{12} + C$	$k_{a2-} \times R_{22}$	$R_{22} \rightarrow R_{22} - 1; R_{12} \rightarrow R_{12} + 1; C \rightarrow C + 1$
$R_{00} + C \rightarrow R_{01}$	$k_{r1+} \times C \times R_{00} / \Omega$	$R_{00} \rightarrow R_{00} - 1; R_{01} \rightarrow R_{01} + 1; C \rightarrow C - 1$
$R_{01} \rightarrow R_{00} + C$	$k_{r1-} \times R_{01}$	$R_{01} \rightarrow R_{01} - 1; R_{00} \rightarrow R_{00} + 1; C \rightarrow C + 1$
$R_{01} + C \rightarrow R_{02}$	$k_{r2+} \times C \times R_{01} / \Omega$	$R_{01} \rightarrow R_{01} - 1; R_{02} \rightarrow R_{02} + 1; C \rightarrow C - 1$
$R_{02} \rightarrow R_{01} + C$	$k_{r2-} \times R_{02}$	$R_{02} \rightarrow R_{02} - 1; R_{01} \rightarrow R_{01} + 1; C \rightarrow C + 1$
$R_{10} + C \rightarrow R_{11}$	$k_{r1+} \times C \times R_{10} / \Omega$	$R_{10} \rightarrow R_{10} - 1; R_{11} \rightarrow R_{11} + 1; C \rightarrow C - 1$
$R_{11} \rightarrow R_{10} + C$	$k_{r1-} \times R_{11}$	$R_{11} \rightarrow R_{11} - 1; R_{10} \rightarrow R_{10} + 1; C \rightarrow C + 1$
$R_{11} + C \rightarrow R_{12}$	$k_{r2+} \times C \times R_{11} / \Omega$	$R_{11} \rightarrow R_{11} - 1; R_{12} \rightarrow R_{12} + 1; C \rightarrow C - 1$
$R_{12} \rightarrow R_{11} + C$	$k_{r2-} \times R_{12}$	$R_{12} \rightarrow R_{12} - 1; R_{11} \rightarrow R_{11} + 1; C \rightarrow C + 1$
$R_{20} + C \rightarrow R_{21}$	$k_{r1+} \times C \times R_{20} / \Omega$	$R_{20} \rightarrow R_{20} - 1; R_{21} \rightarrow R_{21} + 1; C \rightarrow C - 1$
$R_{21} \rightarrow R_{20} + C$	$k_{r1-} \times R_{21}$	$R_{21} \rightarrow R_{21} - 1; R_{20} \rightarrow R_{20} + 1; C \rightarrow C + 1$
$R_{21} + C \rightarrow R_{22}$	$k_{r2+} \times C \times R_{21} / \Omega$	$R_{21} \rightarrow R_{21} - 1; R_{22} \rightarrow R_{22} + 1; C \rightarrow C - 1$
$R_{22} \rightarrow R_{21} + C$	$k_{r2-} \times R_{22}$	$R_{22} \rightarrow R_{22} - 1; R_{21} \rightarrow R_{21} + 1; C \rightarrow C + 1$
$\overset{\text{InsP}_3\text{R}}{C_{\text{ER}}} \rightarrow C$	$v_1 \times \frac{R_{20}}{R_T} \times \frac{[\text{InsP}_3]}{K_D + [\text{InsP}_3]} \times \Omega$	$C \rightarrow C + 1$
$\overset{\text{leak}}{C_{\text{ER}}} \rightarrow C$	$v_2 \times \Omega$	$C \rightarrow C + 1$
$C \rightarrow C_{\text{ER}}$	$v_3 \frac{C^2}{K_3^2 + C^2} \times \Omega$	$C \rightarrow C - 1$

### 3. Cellular Ca<sup>2+</sup> imaging

Determination of calcium changes in hepatocytes was as previously described.<sup>40</sup> Briefly, hepatocytes were plated onto glass coverslips coated with type I collagen and loaded with 3  $\mu\text{M}$  Fura2-AM in modified Williams' medium for 40 min (37 °C, 5% CO<sub>2</sub>). After washing, the coverslips were transferred into a perfusion chamber placed on the stage of a Zeiss inverted microscope (Axiovert 35) and continuously perfused with a saline solution containing (in mM): 20 HEPES, 116 NaCl, 5.4 KCl, 1.8 CaCl<sub>2</sub>, 0.8 MgCl<sub>2</sub>, 0.96 NaH<sub>2</sub>PO<sub>4</sub>, 5 NaHCO<sub>3</sub>, and 1 g/L glucose (pH7.4). Calcium imaging was performed as described previously.<sup>21</sup> Fluorescence images were collected by a charge coupled device camera (Princeton Instruments, Trenton, NJ) digitized and integrated in real time by an image processor (Metafluor, Princeton, NJ).

### 4. Immunofluorescence of type 2 InsP<sub>3</sub>-R

Type 2 InsP<sub>3</sub>-R was detected as described previously.<sup>21</sup> Type 2 InsP<sub>3</sub>-R antibodies were from a polyclonal antibody raised against a synthetic peptide corresponding to the 16 C-terminal residues of the rat type 2 InsP<sub>3</sub> receptor molecule. Secondary antibodies for immunofluorescence were Alexa

Fluor 488 (1:500; IgG-conjugated goat antirabbit antibody) from Molecular Probes (Eugene, OR, USA). Negative control was carried out by omitting the specific primary antibody. The primary antibody was incubated with an excess of the corresponding immunogen peptide before use for the specificity control (data not shown). Cells were mounted using the Slow Fade-Light antifade kit or buffered glycerin.

Images were collected with a confocal microscope (EZC1, Nikon) equipped with a x63 oil-immersion lens (NA=1.4) and processed using IMAGE J software (NA denotes numerical aperture).

## III. RESULTS

### A. Oscillations affected by molecular noise in single cells

The pacemaker mechanism for Ca<sup>2+</sup> oscillations involves free Ca<sup>2+</sup> ions and InsP<sub>3</sub>Rs. As the number of these molecules is rather small in a typical hepatocyte (~15 000 and ~6000, respectively, at basal level), the fluctuations arising from the molecular noise proportional to  $1/\sqrt{N}$  are expected to be quite large. In agreement with this reasoning, the statistical analysis of trains of Ca<sup>2+</sup> spikes in hepatocytes

TABLE II. Parameter values used in the Gillespie's simulations of  $\text{Ca}^{2+}$  oscillations described in Sec. II and in Table I. Units correspond to the deterministic version of the model. In the Gillespie's algorithm, concentrations are replaced by number of molecules. Values in parentheses refer to the simulations of the other isoform of the  $\text{InsP}_3$  receptor shown in Fig. 2.

Parameter	Description	Value
$k_{a1+}$	$\text{Ca}^{2+}$ binding to the first activating site of the $\text{InsP}_3\text{R}$	$350 \mu\text{M}^{-1} \text{s}^{-1}$
$k_{a2+}$	$\text{Ca}^{2+}$ binding to the second activating site of the $\text{InsP}_3\text{R}$	$20\,000 \mu\text{M}^{-1} \text{s}^{-1}$
$k_{a1-}$	$\text{Ca}^{2+}$ dissociation from the first activating site of the $\text{InsP}_3\text{R}$	$3000 \text{s}^{-1}$
$k_{a2-}$	$\text{Ca}^{2+}$ dissociation from the second activating site of the $\text{InsP}_3\text{R}$	$30 \text{s}^{-1}$
$k_{i1+}$	$\text{Ca}^{2+}$ binding to the first inhibiting site of the $\text{InsP}_3\text{R}$	$0.5(0.2) \mu\text{M}^{-1} \text{s}^{-1}$
$k_{i2+}$	$\text{Ca}^{2+}$ binding to the second inhibiting site of the $\text{InsP}_3\text{R}$	$100(20) \mu\text{M}^{-1} \text{s}^{-1}$
$k_{i1-}$	$\text{Ca}^{2+}$ dissociation from the first inhibiting site of the $\text{InsP}_3\text{R}$	$25 \text{s}^{-1}$
$k_{i2-}$	$\text{Ca}^{2+}$ dissociation from the second inhibiting site of the $\text{InsP}_3\text{R}$	$0.2 \text{s}^{-1}$
$\beta$	$\text{Ca}^{2+}$ buffering capacity of the cytoplasm	0.05
$K_D$	Half saturation constant of $\text{InsP}_3$ for its receptor	$0.35 \mu\text{M}$
$v_1$	Maximal rate of $\text{Ca}^{2+}$ release through the $\text{InsP}_3$ receptor	$600 \mu\text{M} \text{s}^{-1}$
$v_2$	$\text{Ca}^{2+}$ leak from the ER	$2 \mu\text{M} \text{s}^{-1}$
$v_3$	Maximal rate of $\text{Ca}^{2+}$ pumping into the ER	$100 \mu\text{M} \text{s}^{-1}$
$K_3$	Half saturation constant of $\text{Ca}^{2+}$ pumping into the ER	$0.1 \mu\text{M}$
$R_T$	Total number of clusters of $\text{InsP}_3\text{Rs}$ considered in the simulations	216
$\Omega$	Parameter of the Gillespie's algorithm allowing to modulate the number of $\text{Ca}^{2+}$ ions	$3 \cdot 10^5$

stimulated by low doses of noradrenaline has shown that the CV of the period comes close to 13%.<sup>9</sup> For larger concentrations of hormone, the CV slightly decreases.

To account for such CVs, one has to consider in the simulations based on the Gillespie's algorithm that the  $\text{InsP}_3\text{R}$  are clustered in groups of  $n$  closely packed channels.<sup>9</sup> These  $n$  channels are assumed to be so close that they are all submitted to the same  $\text{Ca}^{2+}$  environment and thus behave as one megachannel, whose conductance equals  $n$  times the conductance of a single channel. This concept of channel clustering is not new in the field of  $\text{Ca}^{2+}$  dynamics as it was early proposed to explain the characteristics of smaller-scale  $\text{Ca}^{2+}$  increases known as  $\text{Ca}^{2+}$  puffs.<sup>7,11,12,41</sup> Shown in Fig. 1(a) are oscillations obtained when assuming that the  $\text{InsP}_3\text{R}$  are clustered in groups of 25 entities. The number of  $\text{Ca}^{2+}$  ions varies in the range of 10 000–25 000, whereas the number of open receptors oscillates between 0 and  $\sim 4300$ , which suggests that most of the receptors are in an active state at the top of the spike. The limit cycle shown on an  $\sim 100$  period time interval looks rather noisy. The period histogram, however, indicates that the distribution of the periods remains quite narrow with a CV of 14%.

To further quantify the robustness of  $\text{Ca}^{2+}$  oscillations, we evaluated the autocorrelation function that measures the degree of periodicity of the time evolution of a given variable. For noisy periodic systems, the envelope of the function decreases exponentially. The half-life, corresponding to a 50% decrease, yields a measure of the robustness of the oscillations with respect to noise. Figure 1(c) indicates that in the case of the oscillations shown in Fig. 1(a) the half-life is of the order of the period itself. This very rapid phase

diffusion<sup>42</sup> can be related to the fact that the phase of  $\text{Ca}^{2+}$  oscillations does not contain any physiologically relevant information. This is not the case for other rhythmic phenomena in cellular physiology, as for example, circadian rhythms.<sup>43</sup>

Channel clustering is not the only factor affecting the regularity of  $\text{Ca}^{2+}$  oscillations. In particular, the respective amounts of the  $\text{InsP}_3\text{R}$  isoforms could also play a role in this respect. The three isoforms of this receptor/channel differ by their regulatory properties. Hepatocytes mainly express the type 2  $\text{InsP}_3\text{R}$ , which is the most sensitive to  $\text{Ca}^{2+}$  changes. Other cell types express mainly type 1  $\text{InsP}_3\text{R}$  such as most neurons, for example. In general however, the three isoforms are coexpressed within the cells.<sup>13</sup> As compared to  $\text{InsP}_3\text{R}$  type 2, type 1  $\text{InsP}_3\text{R}$  is characterized by a wider bell-shaped curve for the dependence of its open probability on cytosolic  $\text{Ca}^{2+}$ . In consequence, it is differently affected by internal fluctuations. Figure 2(a) shows the results of stochastic simulations of  $\text{Ca}^{2+}$  dynamics relying on  $\text{InsP}_3\text{R}$  type 1. With respect to Fig. 1, only two parameter values characterizing  $\text{Ca}^{2+}$  binding to the inhibitory site of the channel have been modified. As attested by the relatively high CV (18%),  $\text{Ca}^{2+}$  oscillations relying on the type 1  $\text{InsP}_3\text{R}$  are slightly less regular than those relying on the type 2. A close examination of a longer time series uncovers that this is due to the occurrence of smaller amplitude  $\text{Ca}^{2+}$  spikes on an elevated baseline. The existence of such spikes can be ascribed to the fact that inhibition of  $\text{Ca}^{2+}$  is less effective for type 1 than for type 2 receptor. Thus, in stochastic simulations,  $\text{Ca}^{2+}$  ions can more easily dissociate from this site and thereby reopen the channel. From another point of view, it can be seen in the

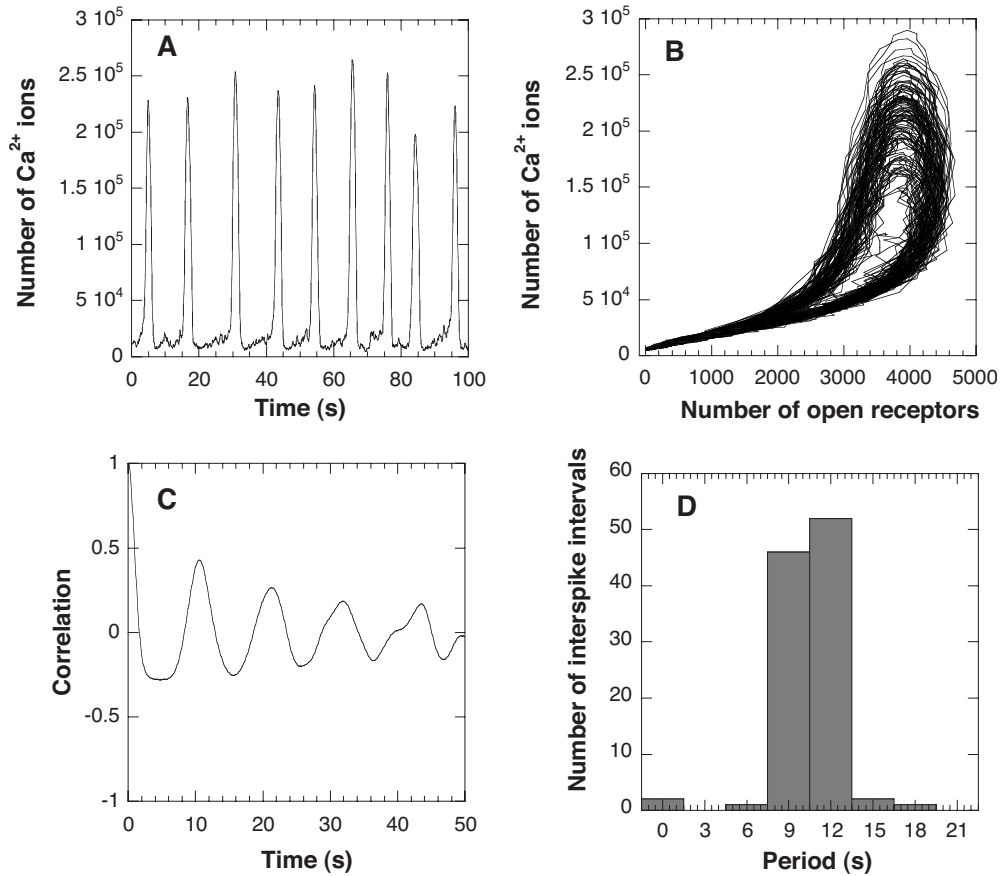


FIG. 1. Gillespie's simulations of Ca<sup>2+</sup> oscillations in hepatocytes. (a) Time series of the number of Ca<sup>2+</sup> ions in the cytoplasm. (b) Phase plane representation of these oscillations. (c) Time evolution of the autocorrelation function for the oscillations shown in panel A. (d) Histogram of the periods calculated for about 100 cycles. Simulations have been performed with the reaction steps shown in Table I and parameters given in Table II with [InsP<sub>3</sub>]=0.1 μM.

phase space that the system tends to quit the proximity of the deterministic limit cycle to undergo small cycles around the unstable steady state (not shown).

In the lower panel of Fig. 2, repetitive spiking occurs for a low level of InsP<sub>3</sub>, in fact corresponding to an excitable system in the deterministic limit. Thus, these oscillations exemplify an autonomous resonance phenomenon.<sup>12,44</sup> Recent experimental evidence for such kind of behavior has been found in hepatocytes.<sup>9</sup> Interestingly, in the case of type 1 InsP<sub>3</sub>R, these noise-induced oscillations appear more regular than those arising at higher InsP<sub>3</sub> levels and are thus in the oscillatory domain (Fig. 2). This observation can be related to the observation that in this domain of parameter values, the CV increases when the period of oscillations decreases, while the opposite generally occurs.<sup>8,9</sup>

### B. Statistical analysis of Ca<sup>2+</sup> oscillations in doublets of connected hepatocytes

Hormonal stimulation of a group of hepatocytes, whose connections through gap junctions remain intact and are thus real fragments of the liver cell plate, induces Ca<sup>2+</sup> increases that are tightly coordinated among the different cells. Such Ca<sup>2+</sup> oscillations are shown in Fig. 3 in the case of two connected cells called a doublet. Both periodic behaviors seem to have approximately the same frequency but are slightly phase shifted.<sup>16,17</sup> The precise mechanism respon-

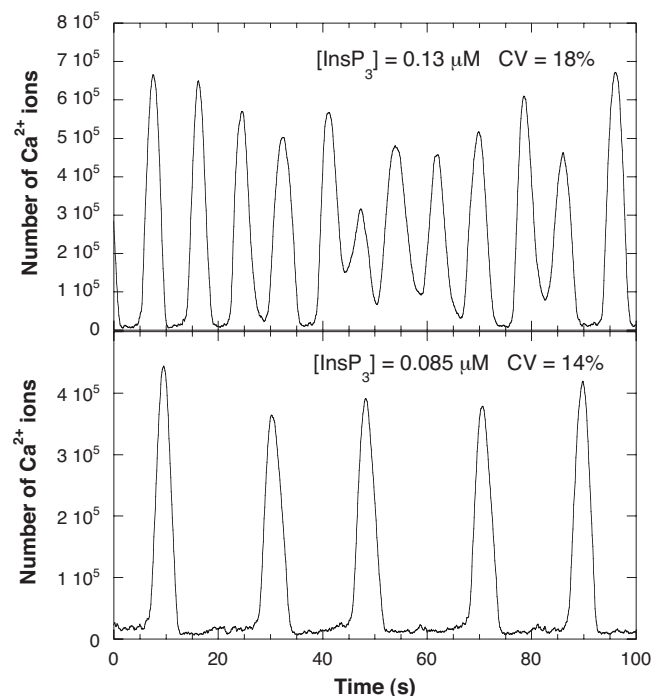


FIG. 2. Effect of changing the regulatory properties of the InsP<sub>3</sub>R in the Gillespie's simulations of Ca<sup>2+</sup> oscillations. Simulations have been performed with the reaction steps shown in Table I and parameters given in Table II considering the values indicated in parentheses.

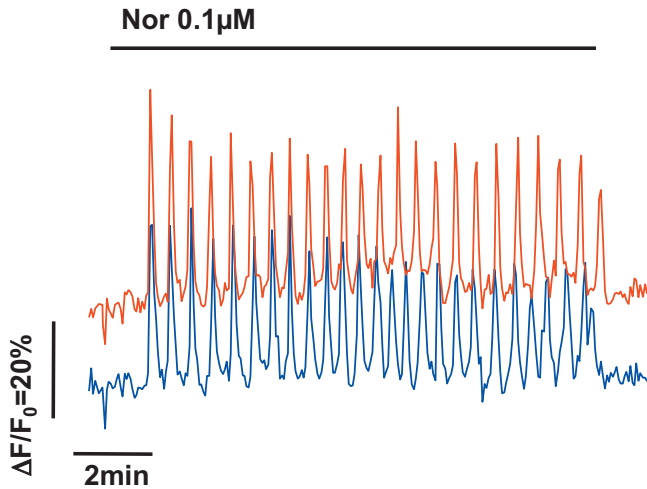


FIG. 3. (Color) Typical  $\text{Ca}^{2+}$  oscillations in two hepatocytes connected by gap junctions and stimulated by  $0.1 \mu\text{M}$  noradrenaline.

sible for this coordinated  $\text{Ca}^{2+}$  spiking is still not fully elucidated mainly because the messenger flowing through the gap junctions ( $\text{InsP}_3$  or  $\text{Ca}^{2+}$ ) cannot be directly identified. Models favoring the hypothesis that  $\text{InsP}_3$  would be the primary coordinating messenger rely on the assumption that there exists among the connected cells a gradient of hormonal sensitivity, i.e., in the number of external receptors to the hormone.<sup>16,17,45</sup> As external receptors are coupled to the enzyme responsible for  $\text{InsP}_3$  synthesis (PLC), this gradient of hormonal sensitivity gives rise to a gradient in the rates of  $\text{InsP}_3$  formation among the different cells. According to this type of models, the direction of the gradient would determine the direction of the wave and its amplitude the propagation velocity. In this model,  $\text{Ca}^{2+}$  does not physically flow from cell to cell, but spiking occurs successively from the most to the less sensitive cell, corresponding to a phase wave.<sup>20</sup> Thus, the interpretation of the behavior shown in Fig. 3 would be the following: the “red cell” called the “leader cell” is more sensitive to noradrenaline and thus synthesizes  $\text{InsP}_3$  at a faster rate and in larger amounts. This cell thus spikes first and successive peaks in this cell have a higher frequency than those in the “blue cell” that synthesizes less  $\text{InsP}_3$ . The differences between the red and blue cells are, however, reduced by the passage of  $\text{InsP}_3$  through gap junctions. The first spikes thus appear only slightly phase shifted in the two cells, while coordination is progressively lost because of the different periods,<sup>20</sup> both oscillators are indeed not really coupled but behave independently with quasisimilar parameter values. In contrast, another model<sup>46</sup> is based on the gap-junctional diffusion of cytosolic  $\text{Ca}^{2+}$ . In this case, for an adequate degree of coupling between cells,  $\text{Ca}^{2+}$  oscillations in connected hepatocytes differing by their structural parameters associated with  $\text{Ca}^{2+}$  dynamics become phase locked. Because of the feedback exerted by  $\text{Ca}^{2+}$  on the  $\text{InsP}_3\text{R}$ , this ion indeed plays a key role in the oscillatory mechanism and dictates the timing of the spikes. Thus, the  $\text{Ca}^{2+}$  increase in one cell will activate the  $\text{InsP}_3\text{Rs}$  in the adjacent coupled cell and a 1:1 phase locking ratio corresponding to synchrony is obtained in the simulations.<sup>46</sup>

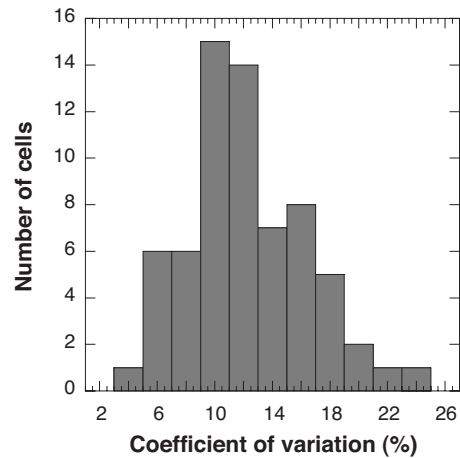


FIG. 4. Histograms of the CVs calculated from experimental time series of  $\text{Ca}^{2+}$  oscillations in doublets of connected hepatocytes stimulated by  $0.1 \mu\text{M}$  noradrenaline. Measurements have been performed on 32 doublets of hepatocytes, i.e., 64 cells, showing at least ten  $\text{Ca}^{2+}$  spikes.

Because of the presence of molecular noise, the discrimination between synchronization and coordination cannot be performed by the simple examination of  $\text{Ca}^{2+}$  time series. Thus, we perform some analyses of experimental  $\text{Ca}^{2+}$  oscillations in doublets of connected hepatocytes to further distinguish between both mechanisms. Following our previous analysis in single hepatocytes,<sup>9</sup> we analyze the time series of oscillations of  $\text{Ca}^{2+}$ -induced fluorescence from doublets of hepatocytes stimulated by  $0.1 \mu\text{M}$  noradrenaline. We only consider traces showing at least ten peaks in both cells. Figure 4 shows the histogram resulting from the analysis of 32 doublets (64 cells). The mean CV equals 12% and the mean period equals 42 s. These values are close to those obtained in our previous study on isolated hepatocytes (13% and 45 s). In the second step, we want to investigate if there were some systematic differences in these quantities for both cells of the doublets. In Fig. 5(a), we have plotted the average period of the less sensitive cell as a function of the period of the most sensitive cell called the leader cell for each doublet. The leader cell is defined as the cell that displays the first  $\text{Ca}^{2+}$  spike. Clearly, the points do not align on the diagonal (shown in light gray), which indicates that both cells of a doublet do not have the same period. The cell that spikes first systematically displays a higher frequency of spiking. Points indeed align pretty well ( $R=0.96$ ) on a line of slope of  $\sim 1$  and ordinate at origin of  $\sim 3$  s [shown in black in Fig. 5(a)]. Thus, these results strongly suggest that  $\text{Ca}^{2+}$  oscillations in doublets of connected hepatocytes are *coordinated* but not *synchronized*. This indirectly corroborates a model based on gap-junctional diffusion of  $\text{InsP}_3$ .

Some more information can be gained from the examination of the regularity of the oscillations in both cells of the doublets. If  $\text{Ca}^{2+}$  spiking were only coordinated by the passage of  $\text{InsP}_3$  through gap junctions, both cells would behave as independent oscillators characterized by roughly the same numbers of  $\text{InsP}_3\text{R}$ . Thus, one would expect the same level of regularity in both the leader and the “less sensitive” cells. In Fig. 5(b), the CV of the less sensitive cell is plotted as a function of the CV of the most sensitive cell for each dou-

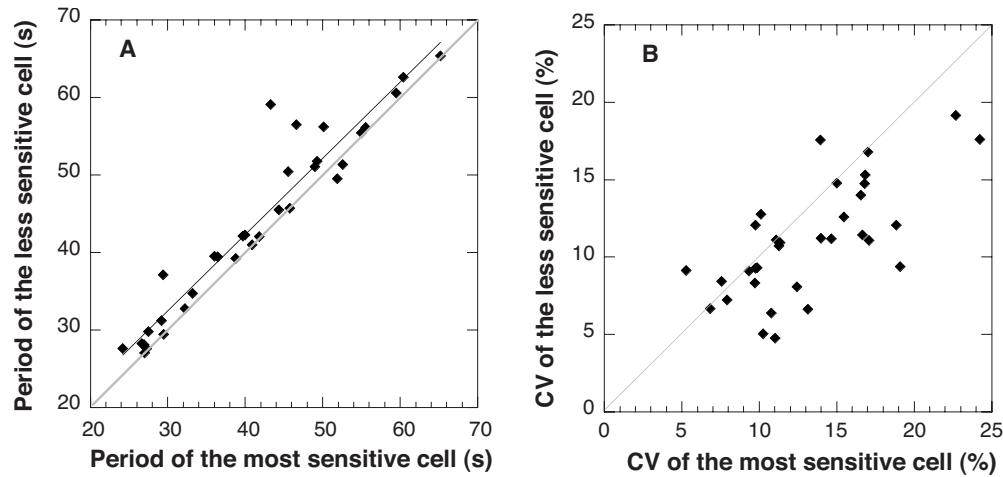


FIG. 5. Statistical analysis of the periods and CVs of the periods in doublets of connected hepatocytes. The most sensitive cell (leader cell) is defined as the cell that shows the first  $\text{Ca}^{2+}$  spike after stimulation. Experimental data are the same as those used in Fig. 4.

blet. As most points are located under the diagonal (shown in light gray), the leader cells have on average a higher CV than the less sensitive cells. In fact, these average values are 13.2% and 11.1% for the most and less sensitive cells, respectively. The larger CVs are associated with the cells having the larger concentration of  $\text{InsP}_3$  and thus the higher frequency. As an increase in  $\text{InsP}_3$  is normally related to a concomitant decrease in both the period and the CV of  $\text{Ca}^{2+}$  oscillations,<sup>8,9</sup> the differences in CVs cannot be ascribed to the differences in  $\text{InsP}_3$  concentrations in both cells of the doublet. Rather, this difference suggests the existence of a mechanism stabilizing the period in the less sensitive connected cell. This could also explain why  $\text{Ca}^{2+}$  oscillations are slightly more regular in doublets of connected hepatocytes than in single cells. Although weak at the level of a doublet, such additional mechanism could be significant at the level of a liver lobule, where tens of cells are coupled by gap junctions and still display a highly coordinated  $\text{Ca}^{2+}$  increase.<sup>18</sup>

#### IV. DISCUSSION

Many excitable and nonexcitable cells display  $\text{Ca}^{2+}$  oscillations when stimulated by a sufficient amount of hormone or neurotransmitter. These oscillations result from the synchronized and periodic opening of a large number of  $\text{InsP}_3$ Rs throughout the cytoplasm. At low levels of hormone or in the absence of stimulation, channels open and close randomly, leading to unsynchronized, small-amplitude and short-duration  $\text{Ca}^{2+}$  increases. Thus, the study of  $\text{Ca}^{2+}$  dynamics offers the fascinating possibility to make the link between microscopic, stochastic events and cellular, highly organized ones. It also allows to investigate the possible role of noise in a prototypic example of spatiotemporal organization at the cellular level. For example, it has been suggested that noise can lead to the extinction of  $\text{Ca}^{2+}$  waves, or, in other conditions, lead to spatially coherent oscillations.<sup>47</sup> On the other hand, results obtained by Prank *et al.*<sup>48</sup> suggest that  $\text{Ca}^{2+}$  spikes can convey faithful information even if extracellular hormonal concentration is perturbed by noise. It has even been proposed that  $\text{Ca}^{2+}$  dynamics always occurs in a sto-

chastic regime: the modeling argument behind this assumption is that a cluster site cannot display oscillations in a deterministic regime.<sup>4,49</sup> Simply speaking, deterministic oscillations cannot occur if the cell would consist of a giant cluster or if the clusters would be spaced very widely. Further work remains to be done to determine the appropriate degree of coupling between cluster sites that would allow the transition from a stochastic to a deterministic regime when increasing the level of stimulation. However, it can be assumed that because of their different intrinsic spatial characteristics,  $\text{Ca}^{2+}$  spiking in different cell types could in fact rely on different dynamics.

In hepatocytes, indirect evidence indicate that  $\text{Ca}^{2+}$  oscillations occur in a deterministic regime.<sup>9</sup> In particular, in a few cells, very irregular  $\text{Ca}^{2+}$  oscillations (CV=31%) can occur for very low levels of stimulation; when increasing very slightly the level of stimulation, the regularity of the  $\text{Ca}^{2+}$  spikes increases abruptly (CV=12%). This observation can be interpreted as the passage through a Hopf bifurcation point, suggesting that for most stimulation levels, oscillations occur in an oscillatory regime. Another study devoted to the modeling of complex  $\text{Ca}^{2+}$  oscillations in the form of bursting or chaos in ATP-stimulated hepatocytes also shows that these spiking patterns can be ascribed to an underlying oscillatory dynamics significantly perturbed by noise.<sup>50</sup> Using the methods of nonlinear time series analysis, a third study<sup>51</sup> concludes in contrast that experimental  $\text{Ca}^{2+}$  traces in hepatocytes are prevalently of stochastic nature. The reported randomness is, however, higher for bursting than for spiking  $\text{Ca}^{2+}$  oscillations. Given the totally different approach used by the last authors, the reasons of the apparent discrepancy between their conclusion and of Dupont *et al.*<sup>9</sup> are hard to pinpoint. However, an obvious difference is that our analysis only takes into account the time intervals between successive  $\text{Ca}^{2+}$  peaks, while Perc *et al.*<sup>51</sup> consider a complete time series of  $\text{Ca}^{2+}$ -induced aequorin bioluminescence.  $\text{Ca}^{2+}$  concentrations at all times are taken into account, while we only consider peak  $\text{Ca}^{2+}$  levels. Thus, fluctuations occurring at basal levels of  $\text{Ca}^{2+}$  are also included in the global analysis of Ref. 51. As basal levels of  $\text{Ca}^{2+}$  are sensitive to external

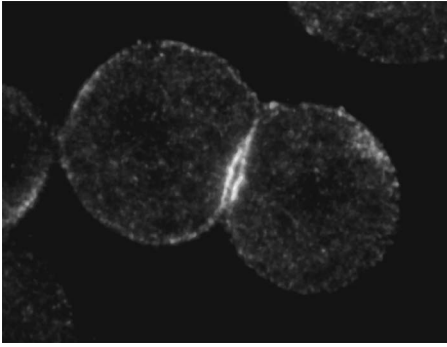


FIG. 6. Visualization of the type 2  $\text{InsP}_3$  receptor labeling in rat hepatocyte doublets. Cells plated on collagen-coated glass coverslips were incubated in the presence of a polyclonal antitype 2  $\text{InsP}_3$  receptor antibody. As shown here, this antibody homogeneously labeled the cytosol, particularly areas around the bile canaliculus domain. Images are representative of 26 doublets examined in three independent experiments.

perturbations, it may be that the higher level of stochasticity predicted by these authors could be, at least in part, related to the noise generated by the environment.

In the present study, we have extended the analysis of the regularity of the  $\text{Ca}^{2+}$  spikes to situations where individual hepatocytes are coupled by gap junctions. The first conclusion that we draw from this analysis is that  $\text{Ca}^{2+}$  spiking between both cells is not synchronized but coordinated. Together with extensive experimental results,<sup>16,17,21,45</sup> this corroborates our assumption that such  $\text{Ca}^{2+}$  spikes among small groups of connected hepatocytes correspond to phase waves due to a gradient in hormonal sensitivity and the passage of  $\text{InsP}_3$  between gap junctions.<sup>20</sup> Interestingly, the present statistical analysis also suggests the existence of a weak entrainment mechanism, as the cell that is less sensitive to the hormonal stimulation displays slightly more regular  $\text{Ca}^{2+}$  oscillations. The molecular nature of this stabilizing mechanism remains unknown but we hypothesize that it could be related to the accumulation of  $\text{InsP}_3\text{R}$  type 2 in the bile canaliculus area, as shown in Fig. 6 (see also Ref. 52). This group of channels could be locally activated by the  $\text{Ca}^{2+}$  peak in the adjacent cell and thereby favors the occurrence of a spike in the connected cell that is anyway close to spiking as both cells have nearly the same amount of  $\text{InsP}_3$ . Further simulations are needed to test if the entrainment by local  $\text{Ca}^{2+}$  could indeed lead to more robust oscillations without giving rise to synchronization. Moreover, it has to be tested if this can be done in conditions that do not induce any significant increase in  $\text{Ca}^{2+}$  at the cell level. It has been shown indeed that a massive increase in cytosolic  $\text{Ca}^{2+}$  in one cell of the doublet does not induce any detectable  $\text{Ca}^{2+}$  rise in the connected cell if the latter is not stimulated.<sup>21</sup> Finally, it would be interesting to test if this effect, which is small at the level of a doublet of cells, could have significant implications at the level of a liver lobule that contains a few tens of hepatocytes. Thus, noise analysis appears as a new dimension in the interplay between experiments and modeling to uncover the molecular mechanisms responsible for the widespread spatiotemporal organization of  $\text{Ca}^{2+}$  dynamics.

## ACKNOWLEDGMENTS

G.D. is Maître de Recherche at the Belgian FNRS. G.D. acknowledges the support from the Fonds de la Recherche Scientifique Médicale (Grant No. 3.4636.04), the European Union through the Network of Excellence BioSim (Contract No. LSHB-CT-2004-005137), and the Belgian Program on Interuniversity Attraction Poles initiated by the Belgian Federal Science Policy Office (Project No. P6/25) (BIOMAGNET). L.C. acknowledges the support from ANR (Grant No. RPV07094LSA) and PNR in Hepatogastroenterology. L.C. is supported by an interface contract between Inserm and AP-HP (LE Kremlin-Bicetre Hospital). This work was supported by a PHC Tournesol 2009 program.

- <sup>1</sup>M. Berridge, M. Bootman, and H. Roderick, *Nat. Rev. Mol. Cell Biol.* **4**, 517 (2003).
- <sup>2</sup>M. Bootman, E. Niggli, M. Berridge, and P. Lipp, *J. Physiol. (London)* **482**, 533 (1997).
- <sup>3</sup>J. Marchant and I. Parker, *EMBO J.* **20**, 65 (2001).
- <sup>4</sup>R. Thul and M. Falcke, *Phys. Biol.* **2**, 51 (2005).
- <sup>5</sup>M. Huertas and G. Smith, *J. Theor. Biol.* **246**, 332 (2007).
- <sup>6</sup>G. Williams, E. Molinelli, and G. Smith, *J. Theor. Biol.* **253**, 170 (2008).
- <sup>7</sup>M. Falcke, *Adv. Phys.* **53**, 255 (2004).
- <sup>8</sup>A. Skupin, H. Kettenman, U. Winkler, M. Wartenberg, H. Sauer, S. Tovey, C. Taylor, and M. Falcke, *Biophys. J.* **94**, 2404 (2008).
- <sup>9</sup>G. Dupont, A. Abou-Lovergne, and L. Combettes, *Biophys. J.* **95**, 2193 (2008).
- <sup>10</sup>A. Spät, P. Bradford, J. McKinney, R. Rubin, and J. Putney, *Nature (London)* **319**, 514 (1986).
- <sup>11</sup>S. Swillens, G. Dupont, L. Combettes, and P. Champeil, *Proc. Natl. Acad. Sci. U.S.A.* **96**, 13750 (1999).
- <sup>12</sup>J. Shuai and P. Jung, *Phys. Rev. Lett.* **88**, 068102 (2002).
- <sup>13</sup>C. Taylor, A. Genazzani, and A. Morris, *Cell Calcium* **26**, 237 (1999).
- <sup>14</sup>E. Vermassen, J. Parys, and J.-P. Mauger, *Biol. Cell* **96**, 3 (2004).
- <sup>15</sup>G. Dupont and L. Combettes, *Biol. Cell* **98**, 171 (2006).
- <sup>16</sup>T. Tordjmann, B. Berthon, M. Claret, and L. Combettes, *EMBO J.* **16**, 5398 (1997).
- <sup>17</sup>T. Tordjmann, B. Berthon, E. Jaquemin, C. Clair, N. Stelly, G. Guillon, M. Claret, and L. Combettes, *EMBO J.* **17**, 4695 (1998).
- <sup>18</sup>L. Robb-Gaspers and A. Thomas, *J. Biol. Chem.* **270**, 8102 (1995).
- <sup>19</sup>A. Nicou, V. Serrière, M. Hilly, S. Prigent, L. Combettes, G. Guillon, and T. Tordjmann, *J. Hepatol.* **46**, 247 (2007).
- <sup>20</sup>G. Dupont, T. Tordjmann, C. Clair, S. Swillens, M. Claret, and L. Combettes, *FASEB J.* **14**, 279 (2000).
- <sup>21</sup>C. Clair, C. Chalumeau, T. Tordjmann, J. Poggioli, C. Erneux, G. Dupont, and L. Combettes, *J. Cell. Sci.* **114**, 1999 (2001).
- <sup>22</sup>I. Bezprozvanny, J. Watras, and B. Ehrlich, *Nature (London)* **351**, 751 (1991).
- <sup>23</sup>E. Finch, T. Turner, and S. Goldin, *Science* **252**, 443 (1991).
- <sup>24</sup>R. Thul, T. Bellamy, H. Roderick, M. Bootman, and S. Coombes, *Adv. Exp. Med. Biol.* **641**, 1 (2008).
- <sup>25</sup>R. Somogyi and J. Stucki, *J. Biol. Chem.* **266**, 11068 (1991).
- <sup>26</sup>A. Atri, J. Amundson, D. Clapham, and J. Sneyd, *Biophys. J.* **65**, 1727 (1993).
- <sup>27</sup>G. Dupont and S. Swillens, *Biophys. J.* **71**, 1714 (1996).
- <sup>28</sup>G. De Young and J. Keizer, *Proc. Natl. Acad. Sci. U.S.A.* **89**, 9895 (1992).
- <sup>29</sup>Y. Tang, J. Stephenson, and H. Othmer, *Biophys. J.* **70**, 246 (1996).
- <sup>30</sup>T. Meyer and L. Stryer, *Annu. Rev. Biophys. Chem.* **20**, 153 (1991).
- <sup>31</sup>G. Dupont and C. Erneux, *Cell Calcium* **22**, 321 (1997).
- <sup>32</sup>A. Politi, L. Gaspers, A. Thomas, and T. Höfer, *Biophys. J.* **90**, 3120 (2006).
- <sup>33</sup>J. Sneyd, K. Tsaneva-Atanasova, V. Reznikov, Y. Bai, M. Sanderson, and D. Yule, *Proc. Natl. Acad. Sci. U.S.A.* **103**, 1675 (2006).
- <sup>34</sup>M. Marhl, S. Schuster, M. Brumen, and R. Heinrich, *Biophys. Chem.* **63**, 221 (1997).
- <sup>35</sup>M. Marhl, M. Gosak, M. Perc, J. Dixon, and A. Green, *J. Theor. Biol.* **252**, 419 (2008).

- <sup>36</sup>U. Kummer, L. Olsen, C. Dixon, A. Green, E. Bornberg-Bauer, and G. Baier, *Biophys. J.* **79**, 1188 (2000).
- <sup>37</sup>M. Kang and H. Othmer, *Phys. Biol.* **4**, 325 (2007).
- <sup>38</sup>A. Le Beau, D. Yule, G. Groblewski, and J. Sneyd, *J. Gen. Physiol.* **113**, 851 (1999).
- <sup>39</sup>D. Gillespie, *J. Comput. Phys.* **22**, 403 (1976).
- <sup>40</sup>G. Dupont, O. Koukoui, C. Clair, C. Erneux, S. Swillens, and L. Combettes, *FEBS Lett.* **534**, 101 (2003).
- <sup>41</sup>J. Shuai, H. Rose, and I. Parker, *Biophys. J.* **91**, 4033 (2006).
- <sup>42</sup>F. Baras, J. E. Pearson, and M. Malek Mansour, *J. Chem. Phys.* **93**, 5747 (1990).
- <sup>43</sup>D. Gonze, J. Halloy, and A. Goldbeter, *Proc. Natl. Acad. Sci. U.S.A.* **99**, 673 (2002).
- <sup>44</sup>H. Li, Z. Hou, and H. Xin, *Phys. Rev. E* **71**, 061916 (2005).
- <sup>45</sup>C. Clair, D. Tran, S. Boucherie, M. Claret, T. Tordjmann, and L. Combettes, *J. Hepatol.* **39**, 489 (2003).
- <sup>46</sup>T. Höfer, *Biophys. J.* **77**, 1244 (1999).
- <sup>47</sup>S. Coombes and Y. Timofeeva, *Phys. Rev. E* **68**, 021915 (2003).
- <sup>48</sup>K. Prank, M. Waring, U. Ahlvers, A. Bader, E. Penner, M. Möller, G. Brabant, and C. Schöfl, *Syst. Biol.* **2**, 31 (2005).
- <sup>49</sup>R. Thul and M. Falcke, *Biophys. J.* **86**, 2660 (2004).
- <sup>50</sup>U. Kummer, B. Krajnc, J. Pahle, A. Green, C. Dixon, and M. Marhl, *Biophys. J.* **89**, 1603 (2005).
- <sup>51</sup>M. Perc, A. Green, J. Dixon, and M. Marhl, *Biophys. Chem.* **132**, 33 (2008).
- <sup>52</sup>K. Hirata, T. Pusch, A. O'Neill, J. Dranoff, and M. Nathanson, *Gastroenterology* **122**, 1088 (2002).